Short thesis for the degree of Doctor of Philosophy (PhD)

Innovative Essential Metal Ion-Based Diagnostic Agents: From Ligand Design to Safer and More Effective In Vivo Applications

by Balázs Váradi

Supervisor: Prof. Dr. Gyula Tircsó full professor

Industrial Consultant: Dr. Zoltán Szűcs

UNIVERSITY OF DEBRECEN

Doctoral School of Chemistry

Debrecen, 2025

I. Introduction and objectives

Early detection and targeted cancer treatment remain among the greatest challenges of modern medicine. Therapeutic strategies increasingly rely on personalized and targeted approaches, including small-molecule drugs, antibody-drug conjugates (ADCs), and cell- and gene-based therapies. These methods not only allow for the selective targeting of tumor cells but also help reduce side effects and improving patients' quality of life.

Accurate and early diagnosis is a prerequisite for advanced targeted therapies, in which molecular imaging plays a crucial role. These techniques enable non-invasive, in vivo visualization of biological processes in living tissues through the use of specific diagnostic molecules. These tracer molecules typically consist of two main components: a targeting moiety (e.g., monoclonal antibody, antibody fragments, peptides, etc.) and a signaling unit that containing a radioisotope.

HER2-positive breast cancer accounts for approximately 15 - 20% of breast tumors, and receptor overexpression is typically associated with a more aggressive clinical course. Reliable - ideally whole-body - determination of HER2 status is fundamental important for personalized care and guiding targeted therapeutic decisions.

Manganese isotopes show great promise for bimodal imaging (PET/MRI - positron emission tomography / magnetic resonance imaging). The isotope ^{52}Mn is a positron emitter ($t_{1/2}$ = 5.59 days) making itsuitable for extended PET scans, particularly when applying slowly circulating, high-molecular-weight vector molecules such as antibodies.

The paramagnetic ^{55}Mn isotope is considered as a potentially safer alternative to gadolinium(III)-based contrast agents for MRI.

The development of Mn(II)-based diagnostic agents lies in the preparation of stable and kinetically inert chelates that ensure long-term stability of the complexes under *in vivo* conditions. The imaging efficiency and selectivity of the tracers depend on the optimized chelator structure and its ability to be conjugated to vector molecules.

The aim of my doctoral research was to developand fine-tune structure of chelators suitable for the complexation of Mn(II) ions, intended for use in modern molecular *in vivo* imaging applications. The following objectives were set:

Development of chelator platform: to design a chelator scaffold capable of forming Mn(II) complex that are suitable for both PET and MRI diagnostics.

Synthesis and study of bifunctional ligands (BFLs): incorporation of the promising chelator scaffold into bifunctional ligands with various donor-atom side chains, enabling systematic investigation of relaxivity, thermodynamic stability, kinetic inertness, and radiolabeling efficiency using ^{52}Mn.

Conjugation of BFLs with biovector molecules, radiolabeling with [^{52}Mn]Mn(II), and in vivo evaluation of the obtained conjugates: attachment of the most promising ligand to a biovector (HER2+ breast cancer-specific antibody or affibody), followed by purification, characterization and assessment of its biological behavior, imaging efficiency, and *in vivo* stability.***Development of a new ligand family through fine-tuning of the chelator scaffold:*** investigation of whether rigidifying the chelator structure and introducing cryptand-like, cross-bridged features can improve the stability and kinetic inertness of Mn(II) complexes. Synthesis of thebifunctional derivatives of these ligands and

characterization of their physicochemical properties systematically compared to identify the structural factors influencing diagnostic performance.

II. Methods

Synthesis: Starting reagents and solvents were purchased from Sigma-Aldrich, Tokyo Chemical Industry, and Fluorochem, and used without further purification. The macrocyclic ligands and their Mn(II) complexes were synthesized by standard synthetic procedures, applying microwave activation (MW) when required (CEM Discover). Reaction monitoring and purification method development were performed by analytical HPLC (Waters Alliance 2690/2695 system equipped with a Waters 996 PDA diode array detector) using reversed-phase columns: Phenomenex Luna C18(2), YMC-Pack ODS-AQ, Waters XBridge Shield RP18. In some cases, intermediate purifications were carried out by flash NP-LC (CombiFlash® EZ Prep), while intermediates and final products were purified by preparative RP-HPLC (YL91100; column: Phenomenex Luna C18(2) preparative). The identity and purity of the obtained compounds were confirmed by $^{1}H/^{13}C$ NMR (Bruker Avance DRX 360 MHz; Bruker Avance I 400 MHz; Bruker Avance II 500 MHz) and HRMS (ESI-QTOF) (Bruker maXis II UHR, coupled to an Agilent 7100 capillary electrophoresis system). XBridge Peptide BEH C18 OBD analytical columns were used for the analysis of protein and conjugate samples, and XBridge Peptide BEH C18 OBD preparative columns were used for their purification.

Equilibrium studies and relaxometry: Protonation constants of ligands and stability constants of the complexes were determined by pH-

potentiometry (Metrohm 785 DMP Titrino). For slowly forming systems (e.g., **3,9-PC2AM^{pip}Bn^{pCO_2H}**), ^{1}H relaxometry using batch samples ("out-of-cell" samples) was applied to determine the stability of the Mn(II) complex. Data fitting was performed using the PSEQUAD program. Relaxivity measurements were carried out with Bruker minispec mq20 (0.47 T) and mq60 (1.41 T) relaxometers at 25.0 and 37.0 °C. r_{1p} and r_{2p} values were calculated from the linear relationship between the measured relaxation rates and Mn(II) concentrations. Relaxometric titrations were also performed (monitoring the pH dependence of relaxation rates R_1, and R_2), in which the diamagnetic contribution of water under the given conditions was subtracted, and the data were normalized to the Mn(II) ion concentration (r_{1p}, and r_{2p})

Kinetic studies: The inertness of PC2A-derived complexes was assessed under the conditions recommended in the literature by P. Caravan et al., where Zn(II)-induced metal exchange was monitored through changes in T_2 relaxation times (1 mM Mn(II) complex; 25 equiv. Zn(II); 37.0 °C; 1.41 T; pH = 6.0; 50 mM MES). For cross-bridged derivatives, acid-assisted dissociation was studied in 0.1 - 1.0 M HCl, using 300 µL sample volume, 1 mM complex, and I = 1.0 M (HCl+NaCl). Reactions were monitored at 25.0 °C and 1.41 T by following T_2 relaxation times.

Production and purification of [^{52}Mn]Mn radioisotope: For radiochemical studies, the ^{52}Mn isotope was produced in a cyclotron by proton irradiation (14 - 18 MeV) of a natural chromium target (^{52}Cr(p,n)^{52}Mn). The manganese produced was purified by anion-exchange chromatography (AG 1-X8), and, when necessary, an additional DGA-based step was applied to remove transition metal contaminants (Fe/Zn/Cu) that could interfere with labeling. The procedures yielded high-purity [^{52}Mn]$MnCl_2$ solutions.

Optimization of [^{52}Mn]Mn radiolabeling and evaluation of transchelation using *trans*-CDTA assays: Radiolabeling conditions of three bifunctional PC2A-derivtive chelators (**3,9-PC2ABn$^{p\text{CO}_2\text{H}}$**, **3,9-PC2MABn$^{p\text{CO}_2\text{H}}$**, **3,9-PC2AM$^{\text{pip}}$Bn$^{p\text{CO}_2\text{H}}$**) were optimized by systematically varying pH (4 - 8), temperature (25 - 95 °C), and ligand concentration (0.3 μM - 1 mM). Reactions were evaluated by analytical RP-HPLC (PDA + Gabi Star RA; column: YMC-Pack ODS-AQ) and iTLC-SG. Transchelation studies were performed in the presence of a large excess of *trans*-CDTA, with sampling at different time points followed by analysis by radio-HPLC. For cryptate-type ligands **3,9-CB$^{8\text{O}2}$PC** and **3,9-CB$^{8\text{O}2}$PCBn$^{p\text{CO}_2\text{H}}$**), radiolabeling was carried out at elevated temperatures (25 and 90 °C), pH 6 - 8, and higher ligand concentrations (1 - 5 mM) due to the slow kinetics of complex formation.
PET/MRI imaging: *In vivo* imaging was conducted in female CB17 SCID mice, using two breast cancer models (4T1 triple-negative murine breast cancer and HER2-positive MDA-MB human breast cancer) implanted at two different anatomical sites (the shoulder region and the inguinal fat pad). The radiopharmaceutical was administered intravenously. Imaging sessions were performed at 4 hours, 1 day, and 3 days post-injection (with an additional 2-day time point for HER2- cases) using a preclinical nanoScan PET/MRI 1T system (Mediso Ltd.). Anesthesia was maintained with inhaled isoflurane throughout the procedures. For MRI, T_1-weighted gradient echo sequences served as anatomical reference. PET data were reconstructed using the MLEM algorithm and analyzed quantitatively based on ROI/VOI (region/volume of interest). Results were expressed as standardized uptake values (SUVs). All animal experiments were carried out under approved protocols, in accordance with EU and national animal welfare regulations (permit number: 16/2020/DEMÁB).

III. New scientific results

III.1. We developed synthetic procedure for the preparation of pyclen-based isomeric ligands (3,6- and 3,9-disubstituted).

Synthetic methods were developed for the synthesis of pyclen-based isomeric ligands (3,6- and 3,9-disubstituted **3,9-PC2A**). In the first step, the **pyclen** (**6**) macrocycle was synthesized, and selective protection of its nitrogen atom (N6) in *trans* position relative to the pyridine unit was achieved by protonation in aqueous medium at pH ≈ 8.55 (**Fig. 1**). Subsequent addition of a stoichiometric amount of the formaldehyde-sodium bisulfite adduct afforded the 3,9-disubstituted product almost quantitatively (with 7% formation of the 3,6-isomer). This intermediate was transformed into the corresponding nitriles (**15**) via NaCN substitution, followed by hydrochloric acid hydrolysis to yield the corresponding diacetates (**16**). The isomeric chelators were purified using preparative HPLC.

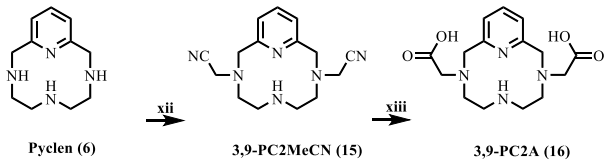

Figure 1. *Synthesis of **3,9-PC2A (16)**:*
(**xii**) $HOCH_2SO_3Na$, H_2O, pH = 8,55, 60 °C → NaCN, RT, 3 h, (**xiii**) conc. HCl, 100 °C, 3 h.

For the preparation of **3,6-PC2A** (**16**), the synthetic procedure involved dialkylation of the previously synthesized **3-Alloc-PC** (**12**) with methyl bromoacetate in the presence of K_2CO_3, cleavage of the Alloc protecting group using $Pd(PPh_3)_4$/phenylsilane, and subsequent acidic hydrolysis of the resulting ester (**18**) (**Fig. 2**).

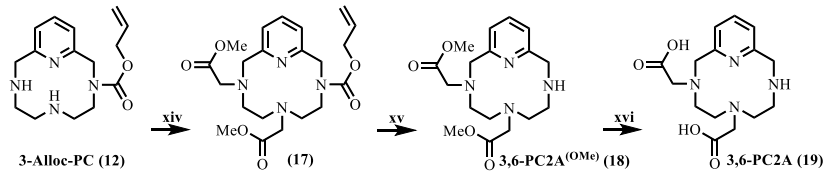

Figure 2. *Synthesis of **3,6-PC2A (19)**:*
(**xiv**) methyl bromoacetate, K_2CO_3, ACN, 20 h (78%); (**xv**) $Pd(PPh_3)_4$, phenylsilane, N_2-atm., CH_2Cl_2, 0 °C → RT, 15 min (64%); (**xvi**) 3 M HCl, 100 °C, 23 h (75%).

III.2. We found that the Mn(II) complexes of 3,6- and 3,9-PC2A exhibit markedly different thermodynamic stability and dissociation behavior, but similar solvent exchange kinetics and relaxation properties.

We investigated the key physicochemical parameters of the Mn(II) complexes of the synthesized ligands. Our results showed that the [Mn(**3,9-PC2A**)] complex has better thermodynamic stability (log K_{MnL} = 17.09(2) vs. 15.53(1) for **3,9-PC2A** and **3,6-PC2A** complexes, respectively) and slightly improved relaxometric properties (r_{1p} = 2.72 and 2.91 $mM^{-1}s^{-1}$ for the **3,6-** and **3,9-PC2A** complexes, respectively, at 25 °C and 0.49 T). These relaxivity values indicate the presence of an inner-sphere water molecule coordinated to the metal ion in both Mn(II) complexes. The [Mn(**3,6-PC2A**)] complex exhibited very reasonable kinetic inertness (k_{obs} = 3.28(3) × 10^{-4} and 5.43(4) × 10^{-4} s^{-1} for the **3,6-** and **3,9-PC2A** complexes, respectively) as determined from Zn(II)-induced metal exchange reactions. Based on these studies, we concluded that both ligands can be treated as suitable platforms for the synthesis of inert Mn(II) complexes and can safely be applied in the design of smart contrast agents or bifunctional ligands. Finally, the 3,9-PC2A ligand platform was selected as the basis for bifunctional ligand design, as the kinetic parameters of its Mn(II) complex can be significantly improved

by introducing electron-withdrawing substituents at the nitrogen atom opposite the pyridine ring (N9).

III.3. We synthesized four bifunctional PC2A derivatives (3,9-PC2ABn^{p}NO$_2$, 3,9-PC2ABn^{p}CO$_2$H, 3,9-PC2MABn^{p}CO$_2$H, 3,9-PC2AM^{pip}Bn^{p}CO$_2$H), to investigate how chemical nature of donor atoms in the side chains influences s the physicochemical parameters of the resulting Mn(II) complexes. In addition, we examined the effect of conjugation-capable moieties (Bn^{p}CO$_2$H, Bn^{p}NO$_2$) on these properties.

Starting from **6-Boc-pyclen** (**14**), the **PC2A$^{(OEt)}$** (**21**) and **PC2MA$^{(OEt)}$** (**23**) derivatives were prepared by dialkylation with ethyl bromoacetate and ethyl-(S)-2-(trifluoromethanesulfonyloxy)propionate, respectively (**Fig. 3**). The Boc protecting group was then removed using a trifluoroacetic acid/dichloromethane mixture.

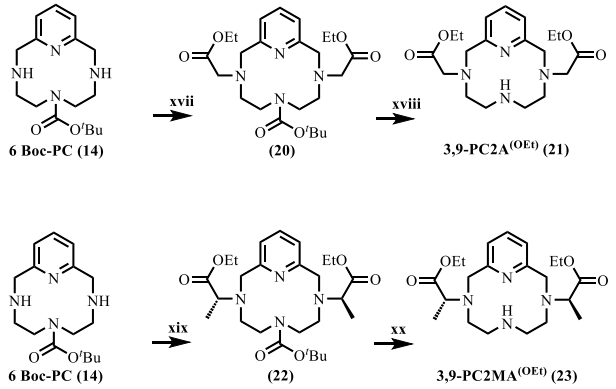

Figure 3. *Synthesis of **3,9-PC2A$^{(OEt)}$** (21) and **3,9-PC2MA$^{(OEt)}$** (23)*:
(**xvii**) ethyl bromoacetate, $CH_3COONa.3H_2O$, ACN, 65 °C, 48 h, (88%); (**xviii**) TFA : DCM (7 : 15), 0 °C → RT, 24 h (93%); (**xix**) ethyl (S)-2-(trifluoromethanesulfonyloxy)propionate, K_2CO_3, DCM, 0 °C, 72 h (79%); (**xx**) TFA : DCM (7 : 15), 0 °C → RT, 24 h (96%).

The **3,9-PC2AM^{pip}** (**24**) ligand was obtained by direct alkylation of **pyclen** (**6**) in acetonitrile in the presence of sodium acetate trihydrate as a base (**Fig. 4**).

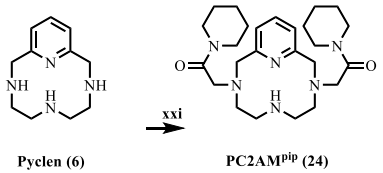

Figure 4. *Synthesis of **3,9-PC2AM^{pip} (24)***:
(**xxi**) 2-bromo-1-(piperidin-1-yl)ethan-1-one, $CH_3COONa.3H_2O$, ACN, 60 °C, 48 h (40%).

Secondary amines at the 6-position were alkylated with *tert*-butyl-4-(bromomethyl)benzoate in the presence of DIPEA, K_2CO_3 or NaI. Subsequent removal of the ester protecting groups afforded BFLs bearing a terminal Bn^{pCO_2H} moiety (**Fig. 5**).

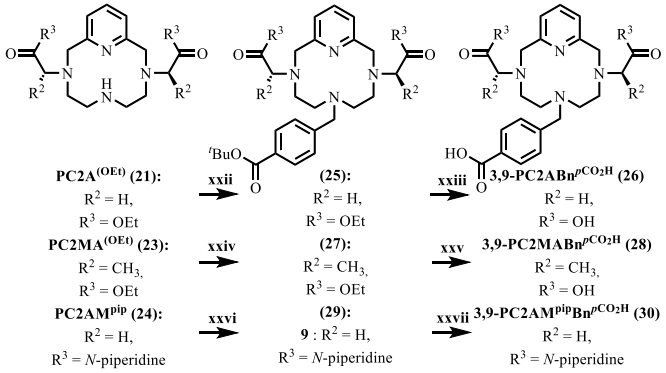

Figure 5. Synthesis of ***3,9-PC2ABn^{pCO_2H} (26)***, ***3,9-PC2MABn^{pCO_2H} (28)*** *and* ***3,9-PC2AM^{pip}Bn^{pCO_2H} (30)***:
(**xxii**) *tert*-butyl 4-(bromomethyl)benzoate, NaI, DIPEA, ACN, 80 °C, 72 h (93%); (**xxiii**) NaOH, EtOH, 60 °C, 3 h (86%); (**xxiv**) *tert*-butyl 4-(bromomethyl)benzoate, NaI, K_2CO_3, ACN, 80 °C, 72 h (52%); (**xxv**) NaOH, EtOH, RT → 60 °C, 3 h (87%);
(**xxvi**) *tert*-butyl-4-(bromomethyl)benzoate, K_2CO_3, ACN, 60 °C, 48 h (84%);
(**xxvii**) TFA : DCM (7 : 15), 0 °C → RT, 12 h (96%).

For the synthesis of the **3,9-PC2ABn^{pNO_2}** ligand, the **3,9-PC2MeCN** (**15**) intermediate was alkylated with *p*-nitrobenzyl bromide, and the resulting product (**31**) was subsequently hydrolyzed with hydrochloric acid (**Fig. 6**).

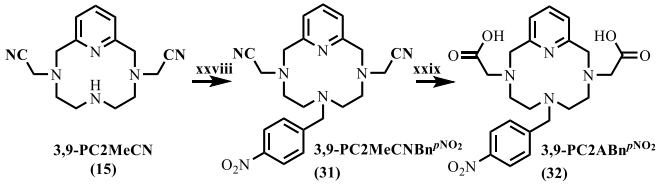

Figure 6. Synthesis of ***3,9-PC2ABn^{pNO_2} (32)***:
(**xxviii**) *p*-nitrobenzyl bromide, NaI, DIPEA, 60 °C, 72 h →
(**xxix**) conc. HCl, 110 °C, 3 h (66%).

III.4. It was found that incorporation of the chelators into the BFL framework led to improved the relaxometric and kinetic properties of the resulting Mn(II) chelates, whereas their thermodynamic stability remained unchanged.

Through the studies of the ligands and their Mn(II) complexes, we demonstrated that the transformation of the parent **3,9-PC2A** chelator into bifunctional ligands improved the dissociation kinetics and relaxometric properties of the Mn(II) complexes, while the apparent stability of the complexes either remained unchanged (acetate side chains) or decreased only slightly (α-methyl-acetate and amide derivatives). The Mn(II) chelate of the nitro-substituted ligand exhibited better kinetic parameters; however, classical reduction reactions led to side products, and therefore the benzoic acid derivative was ultimately chosen for conjugations.

III.5. Based on the results of radiolabeling reactions with [^{52}Mn]Mn(II) we found that macrocyclic BFLs containing carboxylate groups could be labeled instantaneously, whereas efficient labeling of the ligand bearing an amide metal binding moiety required elevated temperatures or prolonged reaction times.

The model bifunctional ligands were labeled with cyclotron-produced and purified [^{52}Mn]Mn(II), and the physicochemical properties of the resulting complexes were investigated. The acetate derivatives were efficiently labeled within 5 min at pH > 6.0, even at 1 μM ligand concentration. In contrast the **3,9-PC2AM^{pip}Bn^{pCO_2H}** bis(amide) derivative ligand required 4 - 5 hours at room temperature or heating to 50 °C to achieve near-quantitative labeling. Notably, the Mn(II) complex of this ligand exhibited the highesrt kinetic inertness, as demonstrated by transchelation experiments in the presence of excess ***trans*-CDTA**. Despite this kinetic advantage, **3,9-PC2ABn^{pCO_2H}** (the carboxylate derivative) was selected for bioconjugation, as the amide side chains of the former hydrolyzed under radiochemical conditions, yielding the corresponding diacetate ligand. Based on these findings s, **3,9-PC2ABn^{pCO_2H}** was selected as the most suitable ligand for the development of the targeted radiotracer candidate.

III.6. A synthetic method for preparing a derivative of the selected BFL (3,9-PC2AM^{pip}Bn^{pCO_2H}) suitable for selective conjugation (3,9-PC2ABn^{pMA}) was developed.

The selected **3,9-PC2AM^{pip}Bn^{pCO_2H}** chelator contains two coordinating acetate groups and a non-coordinating *p*-benzoic acid unit designed for conjugation. Since the chelator possesses the same functional groups for both conjugation and metal binding, instead of direct biovector coupling we introduced a maleimide reactive group on the p-benzoic acid moiety.

To achieve this, , the acetate groups were first protected. The key steps of the synthesis (**Fig. 7**) included alkylation of **3,9-diNs-pyclen** (**13**) with *tert*-butyl-4-(bromomethyl)benzoate; removal of the nosyl protecting groups with thiophenol; introduction of acetate side chains with *tert*-butyl bromoacetate; and introduction of the maleimide reactive group by HBTU/HOBt activation of the carboxyl group of the *p*-benzoic acid unit. Finally, removal of the protecting groups afforded the **3,9-PC2ABnpMA** (**38**) ligand.

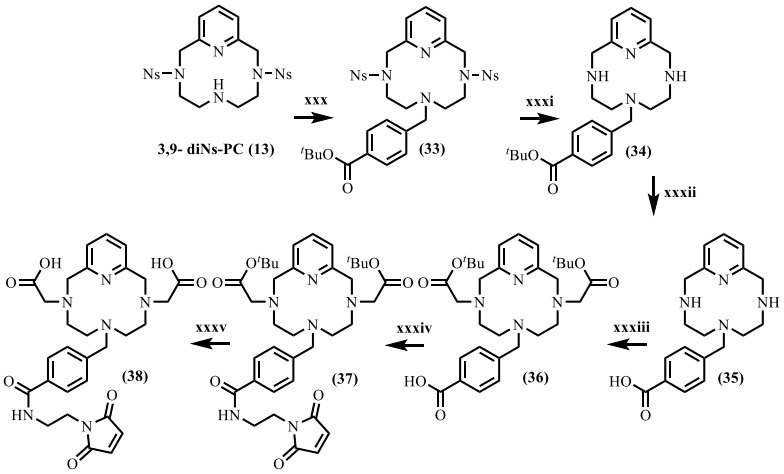

Figure 7. Synthesis of ***3,9-PC2ABn^{pMA} (38)***:
(**xxx**) *tert*-butyl 4-(bromomethyl)benzoate, NaI, DIPEA, ACN, 80 °C, 48 h (93%); (**xxxi**) thiophenol, K_2CO_3, DMF, RT, 24 h (58%); (**xxxii**) TFA : DCM (7 : 15), RT, 12 h (93%); (**xxxiii**) t*ert*-butyl bromoacetate, DIPEA, DMF, 60 °C, 48 h (42%); (**xxxiv**) HBTU, HOBt, DIPEA, DCM, RT, 48 h (56%); (**xxxv**) TFA : DCM (7 : 15), 0 °C → RT, 24 h (90%).

III.7. We optimized the bioconjugation of the 3,9-PC2ABn^{pMA} (38) ligand with an anti-HER2 affibody (43) and performed its radiolabeling with [^{52}Mn]Mn(II) (44).

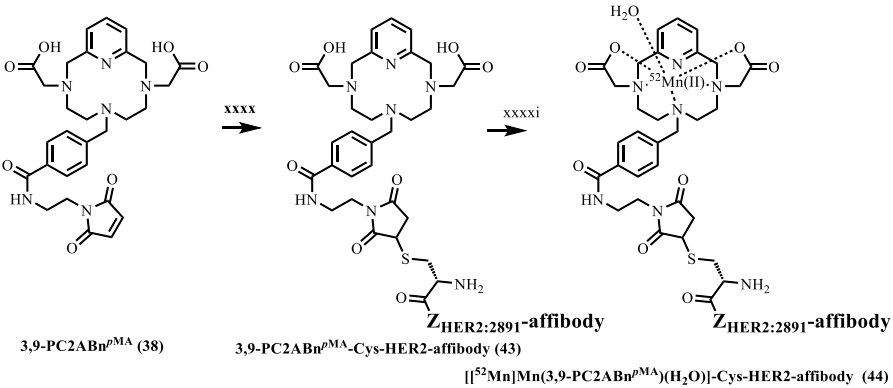

Figure 8. *Conjugation of the bifunctional ligand **(BFL) 3,9-PC2ABn^{pMA} (38)** to an anti-HER2 affibody and preparation of [[^{52}Mn]Mn(**3,9-PC2ABn^{pMA}**)(**H$_2$O**)]-Cys-HER2-affibody **(44)**.* (**xxxx**) 2 mg reduced Z$_{HER2:2891}$-Cys-affibody, 333 µL 1.0 M ammonium acetate (pH = 5.5), 1 mL MQ-water, 60 µL ACN, 37 °C, 5 d; (**xxxxi**): 1.68 - 3.36 MBq [^{52}Mn]MnCl$_2$, 4,35 µmol HEPES (pH = 7.02) puffer, RT, 15 min.

The affibody (Z$_{HER2:2891}$), produced and tested *in vitro* at the Institute of Biochemistry of the Romanian Academy, was purified by RP-HPLC prior to conjugation. Due to the chemoselectivity of thiol-maleimide Michael addition, we optimized the pH of the coupling reaction. Within the literature-reported pH-range (pH 6.5 - 7.5) we observed maleimide hydrolysis and amine addition (**Fig. 8**). Therefore, the reaction was carried out at pH = 5.5, 37 °C, under an argon atmosphere, using 2 mg affibody with an excess amount of **3,9-PC2ABn^{pMA}** (**38**). After five days, more than 98% conversion was achieved. The product was isolated by RP-HPLC, its structure confirmed by ESI-QTOF-UHRMS, and then lyophilized.

III.8. We prepared the radiotracer [^{52}Mn]Mn(3,9-PC2ABn^{pMA})(H$_2$O)-Cys-HER2-affibody (44) by radiolabeling the conjugate with [^{52}Mn]Mn(II).

The conjugate was labeled under previously optimized conditions in HEPES buffer (pH = 7.02) for 15 minutes at room temperature (**Fig. 8**). Following radiolabeling, the sample was diluted to the appropriate volume and used without further purification for in vivo PET/MRI experiments, as the radiotracer was obtained with 100% radiochemical purity, as confirmed by radio-HPLC and iTLC analyses.

III.9. We tested the radiotracer [^{52}Mn]Mn(3,9-PC2ABn^{pMA})(H$_2$O)-Cys-HER2-affibody (44) *in vivo* in CB17 severe combined immunodeficient (SCID) mice bearing MDA-MB (HER2+) and 4T1 (HER2-) tumors.

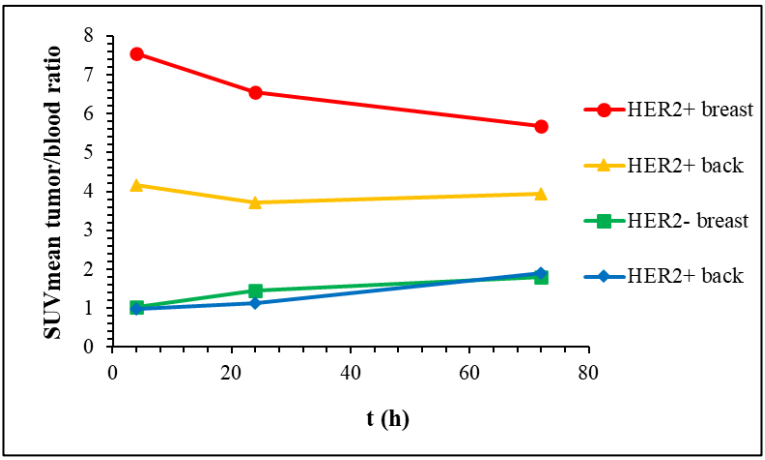

Figure 10. *Time-activity curves (TACs) of the SUVmean tumor-to-blood ratio (mammary and back implants) obtained from serial nanoPET/MR imaging of CB17 SCID mice bearing MDA-MB-HER2$^+$ (HER2+) and 4T1 (HER2-) xenografts following tail-vein injection of the [[^{52}Mn]Mn(**3,9-PC2ABn^{pMA}**)(H$_2$O)]-Cys-HER2-affibody radiotracer.*

Our imaging studies revealed that the produced radiotracer showed remarkable accumulation in HER2-positive tumor tissue as early as 4 hours post-injection as observed in *in vivo* PET/MRI scans (**Fig. 10**). These results demonstrate that the conjugate is suitable for the detection of HER2-positive breast cancer by PET/MRI imaging. We also observed that the specific tumor uptake of lesions implanted in different tissues (muscle/shoulder and inguinal mammary fat pad) varied significantly (**Fig. 9**)indicating that the local tumor microenvironment influences the accumulation of the conjugate. In addition, the radiotracer exhibited high renal clearance, which we aim to reduce in future by introducing human serum albumin (HSA)-binding unit(s) tot he conjugate.

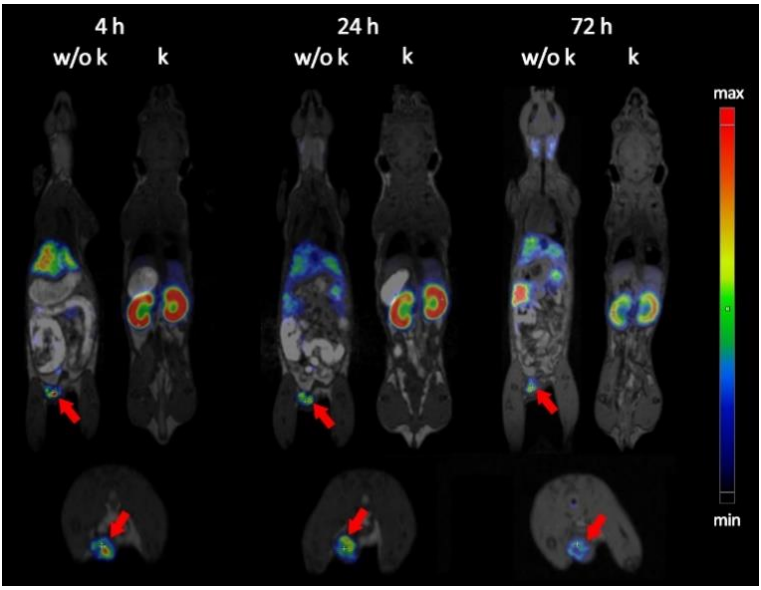

Figure 10. *nanoPET/MR imaging of a CB17 SCID mouse bearing an MDA-MB (HER2+) tumor. Decay-corrected coronal PET images acquired at 4, 24, and 72 h post-injection of the [[52Mn]Mn(**3,9-PC2ABn^{pMA}**)(H_2O)]-Cys-HER2-affibody radiotracer following intravenous (tail-vein) injection (**top**), shown as slices without kidney (**w/o k**) and with kidney (**k**), together with the corresponding transaxial PET images (**bottom**).*
*Orthotopic tumors are indicated by **red arrows**.*

III.10. A novel synthetic route was developed for cryptand derivatives in order to improve the inertness of the Mn(II) chelates.

To enhance the inertness of Mn(II) chelates, we prepared a new family of cryptand ligands based on rigid pyclen, bis-pyclen, and O-pyclen macrocycles. Starting from **6-Boc-pyclen** (**14**), we synthesized the **3,9-CB^{8O2}PC** (**40**) cryptand scaffold via intramolecular ether bridge formation with 1,2-bis(2-iodoethoxy)ethane using sodium acetate sodium acetate trihydrate as a templating base, followed by removal of the Boc protecting group (**Fig. 11**). Subsequent steps, including alkylation with *tert*-butyl-4-(bromomethyl)benzoate and removal of the *tert*-butyl ester protecting groups, yielded a new bifunctional cryptand-type chelator (**42**).

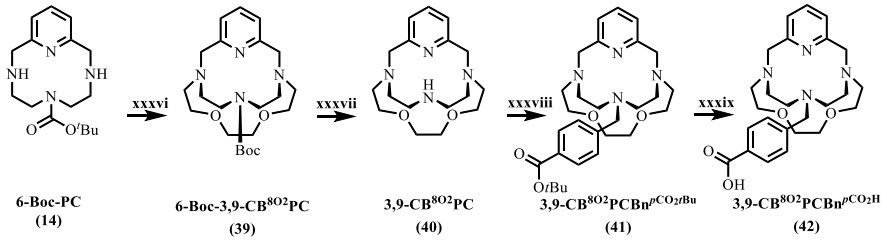

Figure 11. *Synthesis of **3,9-CB^{8O2}PC (40)** and **3,9-CB^{8O2}PCBn^{pCO_2H}(42)**:* (**xxxvi**) 1,2-bis(2-iodoethoxy)ethane, CH3COONa·3H$_2$O, ACN, 110 °C, 48 h (44%); (**xxxvii**) TFA : DCM (7 : 15), 0 °C → RT, 18 h (88%); (**xxxviii**) *tert*-butyl 4-(bromomethyl)benzoate, K$_2$CO$_3$, ACN, 80 °C, 24 h (52%); (**xxxix**) TFA : DCM (7 : 15), 0 °C → RT, 24 h (79%).

III.11. It was determined that the inertness of the Mn(II) complexes formed with the new cryptand-type ligands (3,9-CB^{8O2}PC and 3,9-CB^{8O2}PCBn^{pCO_2H}) closely approaches that of commercially available macrocyclic Gd(III)-based contrast agents.

We investigated the formation and dissociation kinetics, water-exchange and relaxometric properties, as well as the radiolabeling capability of the Mn(II) complexes of the **3,9-CB^{8O2}PC** ligand (a derivative of 3,9-PC2A) and the corresponding bifunctional **3,9-CB^{8O2}PCBn^{pCO_2H}** chelator. We found that the Mn(II) complexes of these cryptand-type ligands form very slowly - taking several days even at pH 7.4 - but exhibit outstanding inertness. Despite their slow formation, [^{52}Mn]Mn-radiolabeling experiments confirmed that these complexes can be efficiently labeled under suitable conditions.

The acid-assisted dissociation rate constant of [Mn(**3,9-CB^{8O2}PCBn^{pCO_2H}**)]$^+$ (k_1 = 1.75 × 10^{-4} M^{-1}s^{-1}) was lower than that of [Gd(**HP-DO3A**)], a commercially available Gd(III)-based macrocyclic contrast agent (k_1 = 6.8 × 10^{-4} M^{-1}s^{-1}), as well as that of the most inert Mn(II) chelate reported to date (k_1 = 1.6 × 10^{-3} M^{-1}s^{-1}). This value approaches that of [Gd(**DO3A-BT**)] contrast agent (k_1 = 2.8 × 10^{-5} M^{-1}s^{-1}). The relaxivity of the Mn(II) chelate of the synthesized BFL ligand was also comparable (r_{1p} = 4.27 mM^{-1}s^{-1}, pH 7.4, 37 °C, 0.49 T) to that of commercially available Gd(III)-based contrast agents such as **DOTAREM** (r_{1p} = 3.4 mM^{-1}s^{-1}) and the withdrawn **MAGNEVIST** (r_{1p} = 3.4 mM^{-1}s^{-1}). Based on their acid-assisted dissociation kinetic properties, [Mn(**3,9-CB^{8O2}PC**)]$^{2+}$ and [Mn(**3,9-CB^{8O2}PCBn^{pCO_2H}**)]$^+$ represent the most inert Mn(II) complexes reported to date. Owing to these exceptional properties, this new ligand family has been placed under patent protection.

IV. Potential applications of the results

The results presented in this dissertation lie at the intersection of applied coordination chemistry and medical imaging. Our findings may have indirect implications for medical diagnostic and therapeutic applications.

The 3,9-PC2A-based bifunctional platform fulfills the requirements of both PET and MRI: chelators with acetate side chains provide rapid and efficient [^{52}Mn]Mn(II) labeling and favorable inertness against transchelation reactions. The relaxometric performance of paramagnetic Mn(II) complexes is clinically relevant. Indeed, GE (General Electric) is currently testing an Mn(II) complex of a PC2A-derived chelator in a phase II clinical trial. The modular benzyl-carboxylate/maleimide anchoring system enables selective conjugation of antibodies, affibodies, and peptides, thus allowing rapid adaptation of the system to other targets (e.g., EGFR, PSMA) while maintaining labeling capacity and imaging performance.

The prepared radiotracer demonstrated measurable, targeted radiotracer accumulation in HER2-positive tumors as early as 4 h after injection in in vivo PET/MRI experiments, supporting its diagnostic value. Differences in tracer uptake between implantation sites (shoulder muscle vs. inguinal mammary fat pad) highlight the influence of the tumor microenvironment on tracer uptake, which may inform future diagnostic and therapeutic strategies . To reduce renal burden and prolong biological half-life, we plan to introduce HSA-binding units, adjust charge/hydrophobicity, and apply optimized linker architectures.

The newly developed Mn(II) complexes of cryptand ligands may offer excellent alternatives to the currently dominant Gd(III)-based MRI

agents in specific respects. Due to their exceptional a Hungarian patent (P2400001) was filed for this ligand family, which was subsequently extended to international protection in 2025.

A promising strategy bridge the sensitivity gap between PET and MRI is the application of a ^{52}/^{55}Mn "cocktail": ^{52}Mn provides the PET signal, while ^{55}Mn contributes paramagnetism, using identical chelation chemistry and conjugation. When attached to a biovector, the effective size of the conjugate increases, leading to a higher rotational correlation time (τ_R), which is expected to improve relaxivity in MRI. In the case of monoclonal antibodies, several (~6 - 7) chelators can be attached to a single biomolecule, further enhancing relaxivity through multivalent effects. Concurrently, HSA-binding units that are capable of binding to human serum albumin (HSA) increase the effective size of the conjugate and decrease rotational correlation speed (i.e., τ_R increases), which further enhances relaxivity. Altogether, these factors may contribute to the development of a truly bimodal PET/MRI conjugate capable of delivering both quantitative molecular (PET) and high-resolution anatomical (MRI) information using the same bioconjugate.

UNIVERSITY of DEBRECEN

UNIVERSITY AND NATIONAL LIBRARY
UNIVERSITY OF DEBRECEN
H-4002 Egyetem tér 1, Debrecen
Phone: +3652/410-443, email: publikaciok@lib.unideb.hu

Registry number: DEENK/461/2025.PL
Subject: PhD Publication List

Candidate: Balázs Váradi
Doctoral School: Doctoral School of Chemistry
MTMT ID: 10063879

List of publications related to the dissertation

Hungarian scientific articles in Hungarian journals (1)

1. **Váradi, B.**, Sajtos, G. Z., Brezovcsik, K., Szűcs, Z., Szedlacsek, S. E., Nagy, G., Tircsó, G.: Mn(II)-alapú diagnosztikai szerek: az alapkutatástól a célzott diagnosztikai eljárásokig.
Sci. Sec. 5 (2), 253-266, 2024. EISSN: 2732-2688.
DOI: http://dx.doi.org/10.1556/112.2024.00208

Foreign language scientific articles in international journals (2)

2. **Váradi, B.**, Brezovcsik, K., Garda, Z., Madarasi, E., Szedlacsek, H., Badea, R. A., Vasilescu, A. M., Puiu, A. G., Ionescu, A. E., Sima, L. E., Munteanu, C. V. A., Călăraş, S., Vágner, A., Szikra, D. P., Ngo, M. T., Nagy, T., Szűcs, Z., Szedlacsek, S. E., Nagy, G., Tircsó, G.: Synthesis and characterization of a novel [52Mn]Mn-labelled affibody based radiotracer for HER2+ targeting.
Inorg. Chem. Front. 10 (16), 4734-4745, 2023. ISSN: 2052-1545.
DOI: https://doi.org/10.1039/D3QI00356F
IF: 6.1

3. Garda, Z., Molnár, E., Hamon, N., Barriada, J. L., Esteban-Gómez, D., **Váradi, B.**, Nagy, V., Póta, K., Kálmán, F. K., Tóth, I., Lihi, N., Platas-Iglesias, C., Tóth, É., Tripier, R., Tircsó, G.: Complexation of Mn(II) by Rigid Pyclen Diacetates: Equilibrium, Kinetic, Relaxometric, Density Functional Theory, and Superoxide Dismutase Activity Studies.
Inorg. Chem. 60 (2), 1133-1148, 2021. ISSN: 0020-1669.
DOI: http://dx.doi.org/10.1021/acs.inorgchem.0c03276
IF: 5.436

DEBRECENI EGYETEM * Egyetemi és Nemzeti Könyvtár *

Patents (1)

4. **Váradi, B.**, Csupász, T., Szilágyi, B., Kapus, I., Sajtos, G. Z., Tircsó, G.: Új kriptát típusú (biciklusos) kelátorok és alkalmazásuk Mn(II)-alapú MRI kontrasztanyagok, Mn-alapú PET diagnosztikai szerek, valamint Cu(II)-izotópra alapozó PET diagnosztikai és terápiás szerek ligandumaiként. 2024
   Hatáskör: Magyarország
   Bejelentés ideje: -
   Ügyiratszám: P2400001 ()
   Szabadalmi szám: P2400001
   Szabadalom státusza: Egyéb

List of other publications

Foreign language scientific articles in international journals (8)

5. Ngo, M. T., Vágner, A., Nagy, G., Ország, G., Nagy, T., Szoboszlai, Z., Csikos, C., **Váradi, B.**, Trencsényi, G., Tircsó, G., Garai, I.: HER2 expression in different cell lines at different inoculation sites assessed by [52Mn]Mn-DOTAGA(anhydride)-trastuzumab.
   Pathol. Oncol. Res. 31, 1-12, 2025. ISSN: 1219-4956.
   DOI: http://dx.doi.org/10.3389/pore.2025.1611999
   IF: 2.3 (2024)

6. Ngo, M. T., Vágner, A., Nagy, G., Ország, G., Nagy, T. M., Csikos, C., **Váradi, B.**, Sajtos, G. Z., Kapus, I., Szoboszlai, Z., Szikra, D. P., Trencsényi, G., Tircsó, G., Garai, I.: [52 Mn]Mn-BPPA-Trastuzumab: A Promising HER2-Specific PET Radiotracer.
   J. Med. Chem. 67 (10), 8261-8270, 2024. ISSN: 0022-2623.
   DOI: http://dx.doi.org/10.1021/acs.jmedchem.4c00344
   IF: 6.8

7. Garda, Z., Szeremeta, F., Quin, O., Molnár, E., **Váradi, B.**, Clémencon, R., Meme, S., Pichon, C., Tircsó, G., Tóth, É.: Small, Fluorinated Mn2+ Chelate as an Efficient 1H and 19F MRI Probe.
   Angew. Chem.-Int. Edit. 63 (43), 1-8, 2024. ISSN: 1433-7851.
   DOI: http://dx.doi.org/10.1002/anie.202410998
   IF: 16.9

8. **Váradi, B.**, Lihi, N., Bunda, S., Nagy, A., Simon, G., Kéri, M., Papp, G., Tircsó, G., Esteban-Gómez, D., Platas-Iglesias, C., Kálmán, F. K.: Physico-Chemical Characterization of a Highly Rigid Gd(III) Complex Formed with a Phenanthroline Derivative Ligand.
   Inorg. Chem. 61 (34), 13497-13509, 2022. ISSN: 0020-1669.
   DOI: http://dx.doi.org/10.1021/acs.inorgchem.2c02050
   IF: 4.6

9. Lucio-Martínez, F., Garda, Z., **Váradi, B.**, Kálmán, F. K., Esteban-Gómez, D., Tóth, É., Tircsó, G., Platas-Iglesias, C.: Rigidified Derivative of the Non-macrocyclic Ligand H4OCTAPA for Stable Lanthanide(III) Complexation.
Inorg. Chem. 61 (12), 5157-5171, 2022. ISSN: 0020-1669.
DOI: http://dx.doi.org/10.1021/acs.inorgchem.2c00501
IF: 4.6

10. Kálmán, F. K., Nagy, V., **Váradi, B.**, Garda, Z., Molnár, E., Trencsényi, G., Kiss, J., Meme, S., Même, W., Tóth, É., Tircsó, G.: Mn(II)-based MRI contrast agent candidate for vascular imaging.
J. Med. Chem. 63 (11), 6057-6065, 2020. ISSN: 0022-2623.
DOI: http://dx.doi.org/10.1021/acs.jmedchem.0c00197
IF: 7.446

11. Guillou, A., Galland, M., Roux, A., **Váradi, B.**, Gogolák, R. A., Le Saëc, P., Faivre-Chauvet, A., Beyler, M., Bucher, C., Tircsó, G., Patinec, V., Maury, O., Tripier, R.: Picolinate-appended tacn complexes for bimodal imaging: Radiolabeling, relaxivity, photophysical and electrochemical studies.
J. Inorg. Biochem. 205, 1-9, 2020. ISSN: 0162-0134.
DOI: http://dx.doi.org/10.1016/j.jinorgbio.2019.110978
IF: 4.155

12. Molnár, E., **Váradi, B.**, Garda, Z., Botár, R., Kálmán, F. K., Tóth, É., Tóth, I., Brücher, E., Tircsó, G.: Remarkable differences and similarities between the isomeric Mn(II)-cis- and trans-1,2-diaminocyclohexane-N,N,N',N'-tetraacetate complexes.
Inorg. Chim. Acta. 472 (1), 254-263, 2018. ISSN: 0020-1693.
DOI: http://dx.doi.org/10.1016/j.ica.2017.07.071
IF: 2.433

Foreign language abstracts (3)

13. Brezovcsik, K., **Váradi, B.**, Tircsó, G., Szűcs, Z.: Examination of bifunctional chelates for efficient labeling of affibodies with 52Mn.
Nucl. Med. Biol. 108-109, S147-S148, 2022. ISSN: 0969-8051.
DOI: http://dx.doi.org/10.1016/S0969-8051(22)00316-X

14. Vágner, A., Ngo, M. T., Nagy, G., Nagy, T., Sajtos, G. Z., **Váradi, B.**, Szikra, D. P., Tircsó, G., Garai, I.: In vivo imaging of HER2 receptor status with a novel Mn-52-labelled antibody.
Eur. J. Nucl. Med. Mol. Imaging. 49 (SUPPL1), S282-S282, 2022. ISSN: 1619-7070.

UNIVERSITY AND NATIONAL LIBRARY
UNIVERSITY OF DEBRECEN
H-4002 Egyetem tér 1, Debrecen
Phone: +3652/410-443, email: publikaciok@lib.unideb.hu

15. **Váradi, B.**, Garda, Z., Madarasi, E., Brezovcsik, K., Vágner, A., Nagy, T., Garai, I., Ngo, M. T., Puiu, A. G., Vasilescu, A. M., Szűcs, Z., Szedlacsek, S. E., Nagy, G., Tircsó, G.: Labelling anti-HER2-affibodies with Mn-52 via pyclen based bifunctional ligands: from ligand design to in vivo PET/MR experiments.
Eur. J. Nucl. Med. Mol. Imaging. 49 (SUPPL1), S283-S283, 2022. ISSN: 1619-7070.

Total IF of journals (all publications): 60,77
Total IF of journals (publications related to the dissertation): 11,536

The Candidate's publication data submitted to the Tudóstér have been validated by DEENK on the basis of the Journal Citation Report (Impact Factor) database.

31 July, 2025

DEBRECENI EGYETEM * Egyetemi és Nemzeti Könyvtár *